Effect of charge fluctuations on the phonon dispersion and electron-phonon interaction in La_2CuO_4

C. Falter, M. Klenner, and W. Ludwig
Institut für Theoretische Physik II-Festkörperphysik, University of Münster, Wilhelm-Klemm-Strasse 10, 4400 Münster, Germany
(Received 6 July 1992; revised manuscript received 11 September 1992)

In this paper we propose a formulation of the electronic density response that is well suited to investigate the influence of localization and delocalization properties of the electrons on the phonon dispersion and the electron-phonon interaction. The formalism is applied to study nonlocal, long-range, electron-phonon-interaction effects of the charge-fluctuation type in high-temperature superconductors, using La_2CuO_4 as an example. Some important features in the experimental phonon spectrum can be understood within such an approach. We discuss the modification of the usual picture of electron pairing, taking into account these nonlocal effects. In this context the symmetric apical oxygen breathing mode at the Z point is of special importance. In this vibration, nonlocal electron-phonon-interaction effects of the charge-fluctuation type are shown to generate in the metallic phase of La_2CuO_4 an interplane charge transfer that is blocked completely in the insulating phase if a strictly two-dimensional electronic structure is assumed. Very recently we became aware of unpublished experimental results where this previously undetected mode appears, unusually broad, as the highest Λ_1 mode at the Z point, in agreement with our theoretical predictions for the insulating phase. Finally, our considerations point towards a simple structure that could be very effective for high-temperature superconductivity.

I. INTRODUCTION

Since the discovery of high-temperature superconductivity[1] in the perovskite-derived copper oxides, many possibilities for its microscopic origin have been discussed. So far there is still no agreement on the mechanism of pairing that is operating in this class of materials. The fact that magnetic, insulating behavior and metallic, superconducting behavior are not separated very much at low temperatures, together with features like CuO planes and strong electron correlations present in these materials, promoted the development of theories with purely electronic and/or magnetic origin. On the other hand, the electron-phonon mechanism was thought to be not strong enough to explain the T_c values in the high-temperature superconductors (HTSC). However, estimates which came to these conclusions exclusively are based on rigid-muffin-tin or more generally on rigid-ion approximations (RIA).[2] The latter take into account only local, short-range changes of the potential felt by an electron if an ion is displaced and ignore nonlocal, long-range contributions. Quite recently *ab initio* calculations have shown that nonlocal contributions to the electron-phonon interaction are quantitatively important for many phonon modes in the HTSC[3] and may even be sufficient to explain the high-T_c value in $YBa_2Cu_3O_7$. Experimental evidence for the important role played by the phonons in the HTSC is, for example, reviewed in Ref. 4. In the present paper we study nonlocal electron-phonon interaction effects typical for the HTSC, using La_2CuO_4 as an example. We investigate their influence on the phonon dispersion and discuss how the usual picture of electron pairing is modified by including these nonlocal effects.

In order that effects of the kind to be discussed in this paper can be observed, certain specific suppositions have to be fulfilled. The latter are realized extremely well in the HTSC but not at all in conventional superconductors. The nonlocal contributions we are talking about have their origin in the anisotropic mixed ionic metallic (covalent) bonding of the HTSC where the metallic component is governed by important localization properties of the electrons introduced in particular by a large electron self-interaction at the copper, leading to restrictions of the mobility of the charge carriers. This is in contrast to the situation found in conventional metals and superconductors based on transition metals which display good metallic screening in all directions of space. The ionic character of bonding, especially in the direction perpendicular to the CuO planes, leads to an anisotropically reduced screening for ions like O_z or La sitting at low-symmetry sites. So it is quite natural to expect that the change in Coulomb potential, induced in particular by the movement of these ions, is not screened nearly as strongly as in the usual high-density metals (note also that there is additionally a change in the on-site potential). The dominant screening mechanism can be supposed to be of charge-fluctuation type and the electron localization effects (correlations) will be important. As a consequence, the movement of an ion leads to nonlocal changes of the potential at the sites of other ions, e.g., in the CuO plane, and causes corresponding charge fluctuations on these ions because of the lack of closed electron shells of the latter, particularly in the metallic regime of the HTSC. In fact, indications of such charge movements have been found for the axial oxygen breathing mode at the Γ point O_z^{Γ} in La_2CuO_4 leading to a charge transfer between in-plane O_{xy} ions and the Cu.[2] See also the discussion of the importance of long-range electron-phonon coupling in HTSC given in Ref. 5.

Compared with the more elaborate direct first princi-

ples calculations in Refs. 2 and 3, our approach is computationally simpler and allows us to calculate the phonon dispersion at all points in the Brillouin zone. In particular, our method was designed to study separately, specific effects of the ionic and metallic component of bonding in the HTSC where the latter is dominated by strong localization properties of the electrons. To take care of such a situation explicitly, a specific description of the displacement-induced change of the electron-density or the density-response function in terms of charge fluctuations and Coulomb interactions is essential. This is achieved by parametrizing the electronic charge density by a suitable set of effective electronic degrees of freedom, e.g., charge fluctuations, and using density-functional theory to calculate how these degrees of freedom change when the ions are displaced. Another point of our approach is that we can discriminate the density response of a metal from that of an insulator by a general criterion that can be used to study directly the effects of a metal-insulator transition on the phonon dispersion.

In the present work, the local part of the electronic density response, which generally is represented by a RIA or in the framework of the quasi-ion approach (QIA)[6–9] by a rigid quasi-ion model, will be described by a suitable *ab initio* ionic model of rigid ions. Then, using such a model as a reference system, nonlocal contributions to the density response in the form of charge fluctuations on the ions are additionally taken into account and their influence on the phonon dispersion is studied. Some important features in the experimental phonon spectrum can be understood within such an approach, supporting the proposed screening mechanism on the basis of charge fluctuations.

In Sec. II, the theoretical method is established and a proper representation for the electronic density-response function, the dynamical matrix, and the electron-phonon matrix elements is derived. The definite modeling of the theory is described in Sec. III, where the results are discussed and conclusions given.

II. THEORETICAL CONSIDERATIONS

In this section, the displacement-induced change of the electron density and the density-response function are expressed in terms of effective electronic degrees of freedom and it is shown how these quantities enter the dynamical matrix and the matrix elements of the electron-phonon interaction.

A. Density response in terms of effective electronic degrees of freedom

The fundamental quantity to describe the phonon dispersion as well as the electron-phonon interaction in a crystal microscopically is the change in density of the electrons at space point $\mathbf{r}$, if an ion located at $\mathbf{R}^{\mathbf{A}}=\mathbf{R}^{\mathbf{a}}+\mathbf{R}^{\alpha}$ ($\mathbf{a},\alpha$, primitive and nonprimitive lattice index, respectively) is displaced in a certain direction. In the adiabatic approximation, this change in density is related to the static density-response function $D(\mathbf{r},\mathbf{r}')$ and the potential of the ion cores $V_\alpha(\mathbf{r}-\mathbf{R}^{\mathbf{A}})$ by[6,7]

$$P_i^{\mathbf{A}}(\mathbf{r})=\int dV' D(\mathbf{r},\mathbf{r}')V_i^{\alpha}(\mathbf{r}'-\mathbf{R}^{\mathbf{A}}) , \tag{1a}$$

with

$$V_i^{\alpha}(\mathbf{r}-\mathbf{R}^{\mathbf{A}})=\frac{\partial}{\partial R_i^{\mathbf{A}}}V_\alpha(\mathbf{r}-\mathbf{R}^{\mathbf{A}}) . \tag{1b}$$

$\mathbf{P}^{\mathbf{A}}(\mathbf{r})$ enters the phonon dispersion via the dynamical matrix $t^{\alpha\beta}(\mathbf{q})$ (Ref. 6).

$$t_{ij}^{\alpha\beta}(\mathbf{q})=(M_\alpha M_\beta)^{-1/2}\left[\phi_{ij}^{\alpha\beta}(\mathbf{q})-\delta_{\alpha\beta}\sum_\gamma \phi_{ij}^{\alpha\gamma}(\mathbf{0})\right] . \tag{2}$$

$\mathbf{q}$ is a wave vector from the first Brillouin zone and M_α is the mass of the ion of type α. $\phi^{\alpha\beta}(\mathbf{q})$ can be decomposed into a direct ion-ion contribution $\phi_{\mathbf{I}}^{\alpha\beta}(\mathbf{q})$, which can be dealt with by the Ewald method and into an electron-mediated contribution $\phi_E^{\alpha\beta}(\mathbf{q})$, which is given by the Fourier-transformed expressions of $\mathbf{P}^{\mathbf{A}}$ and $V_i^{\alpha}(\mathbf{r}-\mathbf{R}^{\mathbf{A}})$, respectively:

$$\phi_{Eij}^{\alpha\beta}(\mathbf{q})=\frac{1}{V_c}\sum_{\mathbf{G}} V_i^{\alpha}(\mathbf{q}+\mathbf{G})^* P_j^{\beta}(\mathbf{q}+\mathbf{G}) \times e^{-i\mathbf{G}\cdot(\mathbf{R}^{\beta}-\mathbf{R}^{\alpha})} . \tag{3}$$

$\mathbf{G}$ is a vector of the reciprocal lattice and V_c the volume of the elementary cell.

In order to describe the displacement-induced change of the electron density $\mathbf{P}^{\mathbf{A}}$ or the density-response function, we introduce effective electronic degrees of freedom (EDF), for example, charge fluctuation, at the ions. We imagine that the electronic charge density ρ is parametrized by a set of suitable "generalized coordinates" representing the EDF: $\zeta=\{\cdots\zeta_\kappa^{\mathbf{a}}\cdots\}$. $\mathbf{a}$ specifies the elementary cells in the crystal and κ numbers the localization centers of the EDF in a certain elementary cell. So we have

$$\rho=\rho(\mathbf{r},\zeta) . \tag{4}$$

The ζ's may be identified, for example, in the framework of the QIA as localization centers ($\rightarrow$"bond charge coordinates"), decay constants ($\rightarrow$"breathing coordinates"), or amplitudes ($\rightarrow$"charge-fluctuation coordinates") of the Gaussians defining the quasi-ion density.

From its definition the displacement-induced change in density $\mathbf{P}^{\mathbf{A}}$ then can be expressed as

$$\mathbf{P}_\alpha^{\mathbf{a}}(\mathbf{r})=\frac{\partial\rho(\mathbf{r})}{\partial\mathbf{R}_\alpha^{\mathbf{a}}}=\sum_{\mathbf{b}\kappa}\frac{\partial\rho(\mathbf{r})}{\partial\zeta_\kappa^{\mathbf{b}}}\frac{\partial\zeta_\kappa^{\mathbf{b}}}{\partial\mathbf{R}_\alpha^{\mathbf{a}}} \equiv-\sum_{\mathbf{b}\kappa}\rho_\kappa(\mathbf{r}-\mathbf{R}_\kappa^{\mathbf{b}})\mathbf{X}_{\kappa\alpha}^{\mathbf{ba}} . \tag{5}$$

A definite model is obtained from Eq. (5) by specifying the form factors ρ_κ of the charge-density variation and the quantities $\mathbf{X}_{\kappa\alpha}^{\mathbf{ba}}$ which describe the reaction of the EDF $\zeta_\kappa^{\mathbf{b}}$ with respect to the displacement of the ion $\mathbf{A}=\mathbf{a}\alpha$.

In earlier studies within the QIA[6,7] the nonlocal (distortion) contributions to $\mathbf{P}^{\mathbf{A}}$ or $\mathbf{X}_{\kappa\alpha}^{\mathbf{ba}}$, respectively, have been simulated explicitly in the form of "rotations" or "breathing" of the quasi-ions and this choice was guided by microscopic calculations of the density-response func-

tion itself. On the other hand, the correct description of $\mathbf{X}$ and in particular its nonlocal part, follows from the minimum principle for the energy,

$$E(\zeta,R)=\tilde{E}[\rho(\zeta),V(R)] , \tag{6a}$$

with respect to the EDF ζ for a given configuration R of the ions. $\tilde{E}$ is the energy functional of density-functional theory,

$$\tilde{E}[\rho]=\int dV\rho(\mathbf{r})V(\mathbf{r},R)+F[\rho] , \tag{6b}$$

$$F=T_s+E_H+E_{\rm xc} . \tag{6c}$$

$V(R)$ is the (external) potential of the ions in the crystal; T_s, E_H, and $E_{\rm xc}$ are the kinetic-, Hartree-, and exchange-correlation energy functionals. This yields $\zeta(R)$ and finally $\mathbf{X}$ by differentiation; see Eq. (5). The (adiabatic) minimization condition can be stated as

$$\left.\frac{\partial E}{\partial\zeta}\right|_{(\zeta(R),R)}=0 , \tag{7}$$

where we have assumed that the definite choice of the ζ and ρ_κ does not violate particle conservation. In a formal but obvious notation, Eq. (7) yields for $(-\mathbf{X})\equiv\zeta'$ after differentiating with respect to the ionic positions R:

$$\zeta'=-(E_{\zeta\zeta})^{-1}E_{\zeta R} . \tag{8}$$

Here and in the following, a shorthand notation for the derivatives has been used, e.g., $E_{\zeta R}\equiv\partial^2E/\partial\zeta\partial R$ etc. The partial derivatives of the energy in Eq. (8) can be represented microscopically in the framework of density-functional theory. In our symbolic notation, we obtain for $\mathbf{P}^{\mathbf{A}}$ and the density-response function D

$$\begin{aligned}P\equiv DV_R&=-\rho_\zeta(E_{\zeta\zeta})^{-1}E_{\zeta R}\\&=-\rho_\zeta(\rho_\zeta F_{\rho\rho}\rho_\zeta)^{-1}\rho_\zeta V_R\end{aligned} \tag{9}$$

and

$$D=-\rho_\zeta(\rho_\zeta F_{\rho\rho}\rho_\zeta)^{-1}\rho_\zeta\equiv-\rho_\zeta(C^{-1})_{\zeta\zeta}\rho_\zeta . \tag{10}$$

Written in full notation the expression for the density-response function is

$$D(\mathbf{r},\mathbf{r}')=-\sum_{\substack{\mathbf{a},\mathbf{b}\\ \kappa,\kappa'}}\rho_\kappa(\mathbf{r}-\mathbf{R}^{\mathbf{a}}_\kappa)(C^{-1})^{\mathbf{ab}}_{\kappa\kappa'}\rho_{\kappa'}(\mathbf{r}'-\mathbf{R}^{\mathbf{b}}_{\kappa'}) , \tag{11}$$

with

$$C^{\mathbf{ab}}_{\kappa\kappa'}=\int dV\,dV'\rho_\kappa(\mathbf{r}-\mathbf{R}^{\mathbf{a}}_\kappa)F''(\mathbf{r},\mathbf{r}')\rho_{\kappa'}(\mathbf{r}'-\mathbf{R}^{\mathbf{b}}_{\kappa'}) \tag{12}$$

and

$$\begin{aligned}F''(\mathbf{r},\mathbf{r}')&=T_s''(\mathbf{r},\mathbf{r}')+v(\mathbf{r}-\mathbf{r}')-v_{\rm xc}(\mathbf{r},\mathbf{r}')\\&\equiv T_s''(\mathbf{r},\mathbf{r}')+\tilde{v}(\mathbf{r},\mathbf{r}') ,\end{aligned} \tag{13}$$

where v is the Coulomb interaction and T_s'' and $(-v_{\rm xc})=E''_{\rm xc}$ are the second functional derivatives with respect to the density ρ of the kinetic energy and the exchange-correlation energy. If we introduce the polarizability π of the electronic system by the relation $\pi^{-1}(\mathbf{r},\mathbf{r}')=T_s''(\mathbf{r},\mathbf{r}')$, we can express C^{-1} in Eq. (11) in compact notation as

$$C^{-1}=(\pi^{-1}+\tilde{V})^{-1}=(1+\pi\tilde{V})^{-1}\pi=\pi(1+\tilde{V}\pi)^{-1} , \tag{14}$$

where $(\pi^{-1})^{\mathbf{ab}}_{\kappa\kappa'}$ and $\tilde{V}^{\mathbf{ab}}_{\kappa\kappa'}$ are defined analogously to $C^{\mathbf{ab}}_{\kappa\kappa'}$ in Eq. (12) with $F''(\mathbf{r},\mathbf{r}')$ replaced by $\pi^{-1}(\mathbf{r},\mathbf{r}')$ and $\tilde{v}(\mathbf{r},\mathbf{r}')$, respectively.

Physically, $C^{\mathbf{ab}}_{\kappa\kappa'}$ means the interaction energy between the form factors $\rho^{\mathbf{a}}_\kappa$ if the corresponding EDF $\zeta^{\mathbf{a}}_\kappa$ have been excited by the displacement of the ions.

Equation (9) can be rewritten as [compare with Eq. (5)]

$$P_i^{\mathbf{A}}(\mathbf{r})=-\sum_{\mathbf{b}\kappa}\rho_\kappa(\mathbf{r}-\mathbf{R}^{\mathbf{b}}_\kappa)X^{\mathbf{bA}}_{\kappa i} , \tag{15}$$

with

$$X^{\mathbf{bA}}_{\kappa i}=\sum_{\mathbf{b}'\kappa'}(C^{-1})^{\mathbf{bb}'}_{\kappa\kappa'}B^{b'\kappa'\mathbf{A}}_{\quad i} \tag{16}$$

and

$$B^{\mathbf{b}\kappa\mathbf{A}}_{\quad i}\equiv\int dV\,\rho_\kappa(\mathbf{r}-\mathbf{R}^{\mathbf{b}}_\kappa)V_i^\alpha(\mathbf{r}-\mathbf{R}^{\mathbf{A}}) . \tag{17}$$

The quantity $(-B^{\mathbf{b}\kappa\mathbf{A}}_{\quad i})$ expresses the "force" on the EDF with form factor ρ_κ located at $\mathbf{R}^{\mathbf{b}}_\kappa$ if ion $\mathbf{A}$ is displaced in the i direction or, equivalently, the "force" on ion $\mathbf{A}$ in the i direction if the EDF $\mathbf{b}\,\kappa$ is excited by a unit excitation. Thus the following picture arises for $\mathbf{P}^{\mathbf{A}}$. The displacement of an ion $\mathbf{A}$ exerts a force on the EDF, so the latter get excited and interact with each other via F'' as described in Eq. (12).

B. Representation of the electron-phonon interaction

Next we outline how the EDF enter the expression of the matrix elements M of the electron-phonon interaction. Following Ref. 6, the matrix elements are given by

$$\begin{aligned}M^\sigma_{\mathbf{k}n,\mathbf{k}'n'}=\sum_{\mathbf{A}i}&\left[\frac{\hbar}{2NM_\alpha\omega_\sigma(\mathbf{q})}\right]^{1/2}e^{i\mathbf{q}\cdot\mathbf{R}^{\mathbf{A}}}\\&\times e_i^\alpha(\mathbf{q}\sigma)\langle\mathbf{k}n|\tilde{V}_i^{\mathbf{A}}|\mathbf{k}'n'\rangle .\end{aligned} \tag{18}$$

$\omega_\sigma(\mathbf{q})$ and $\mathbf{e}^\alpha(\mathbf{q}\sigma)$ denote the phonon frequencies and corresponding eigenvectors for the mode with wave vector $\mathbf{q}$ and polarization σ for an ion of type α. $|\mathbf{k}n\rangle$ symbolize the wave functions of the electrons with wave vector $\mathbf{k}$ and band index n. $\tilde{V}_i^{\mathbf{A}}(\mathbf{r})$ is the change (per unit displacement of the $\mathbf{A}$ atom in the i direction) of the self-consistent potential felt by an electron at space point $\mathbf{r}$.

According to Ref. 6, $\tilde{V}_i^{\mathbf{A}}$ can be related to $P_i^{\mathbf{A}}$ as follows:

$$\tilde{V}_i^{\mathbf{A}}=V_i^{\mathbf{A}}+\tilde{v}P_i^{\mathbf{A}} . \tag{19}$$

$V_i^{\mathbf{A}}$ denotes the (negative) gradient of the bare ion potential. The second (electron mediated) contribution in Eq. (19) is determined by the specific characteristics of the underlying screening mechanism (in our model, of charge-fluctuation type, see Sec. III). Substituting in Eq. (18) and using Eq. (15) we arrive at

$$EM^\sigma_{\mathbf{k}n,\mathbf{k}'n'}=\sqrt{N}\sum_{\mathbf{G},\kappa}\delta\zeta_\kappa^{(\mathbf{q}\sigma)}\langle\mathbf{k}n|\tilde{v}\rho^0_\kappa|\mathbf{k}'n'\rangle\delta_{\mathbf{k}'-\mathbf{k}+\mathbf{q},\mathbf{G}} , \tag{20}$$

with

$$\delta\zeta_\kappa^{(\mathbf{q}\sigma)}=-\sum_{\alpha i}\left[\frac{\hbar}{2M_\alpha\omega_\sigma(\mathbf{q})}\right]^{1/2}e_i^\alpha(\mathbf{q}\sigma)X_i^{\kappa\alpha}(\mathbf{q})e^{i\mathbf{q}\cdot\mathbf{R}^\kappa}\ . \quad (21)$$

$X_i^{\kappa\alpha}(\mathbf{q})$ is the Fourier transform of $X_{\kappa i}^{\mathrm{bA}}$ from Eq. (16). $\delta\zeta_\kappa^{(\mathbf{q}\sigma)}$ means the change of the EDF ζ_κ in the phonon mode $(\mathbf{q}\sigma)$. Note also that for a calculation of the electron-phonon coupling strength λ within the BCS theory of superconductivity, $\mathbf{k}$ and $\mathbf{k}'$ in Eq. (20) have to be kept on the Fermi surface.[10]

III. MODELING OF THE THEORY AND DISCUSSION

We start with the construction of our *ab initio* ionic reference model followed by a calculation of the structure parameters and the phonon dispersion of La_2CuO_4 in this model. Typical features of the dispersion related to the ionic forces are singled out. Then the charge-fluctuation degrees of freedom are implemented and the density response of a metal is discriminated from that of an insulator by a general criterion. The phonon dispersion including the charge fluctuations is then calculated and several characteristic effects of the latter on the dispersion are discussed and compared with the ionic reference system. Results for both the metallic and the (fictitious) insulating phase are presented. Finally, we demonstrate the relevance of nonlocal electron-phonon interaction effects of the charge-fluctuation type for the axial O_z- and La_z-breathing modes at the Γ and Z points and indicate how the usual picture of electron pairing has to be modified by including these nonlocal effects.

A. Construction of the ionic model

In the following the local part of the electronic density response will be approximated explicitly by a proper *ab initio* model of rigid ions to describe the effects of the ionic forces in the crystal. Using such a model as a reference system, we additionally incorporate implicitly nonlocal contributions in the form of charge fluctuations on the ions into the density response by treating these fluctuations as a special type of EDF, according to the method presented in Sec. II. Consequently, Eq. (15) only accounts for the contribution of the charge-fluctuation degrees of freedom to the density response. The contribution of the ion cores $\phi_I^{\alpha\beta}(\mathbf{q})$ in the dynamical matrix then has to be replaced by the contribution of pair potentials $\phi_{\alpha\beta}(R)$, defined below, between the rigid ions of our model. The *ab initio* character of the ionic reference model is important because empirical elements of a reference system, e.g., by fitting a phenomenological model to the experiments, could cover the characteristic features related to the nonlocal electron-phonon interactions we intend to investigate.

The (spherical) ionic densities $\rho_\alpha^{\mathrm{a}}(\mathbf{r})$ of the model have been calculated with a modified Herman-Skillman program,[11] where the Slater exchange potential has been replaced by the exchange potential of local density-functional theory and a correlation potential according to Ref. 12 has been taken into account additionally.

Also an averaged correction for self-interaction effects[12] has been used. The O^{2-} ion, which is unstable in the free state, is stabilized in the crystal by the long-range electrostatic (Madelung) potential of the surrounding neighbors. This effect is modeled by enclosing the oxygen ion in a (Watson) sphere[13] with opposite charge. The radius of the sphere is fixed to give the Madelung potential at the site of the O^{2-} ion in the crystal.

Given these ionic densities, the interactions between the ions are calculated using the approach as proposed by Gordon and Kim,[14] who assumed that the density of a pair of ions is given by overlapping spherical ions. Then the energy of the ion pair is calculated by local-density approximation (LDA), taking for the kinetic contribution the Thomas-Fermi approximation. This results in pair potentials between ions of type α and β:

$$\phi_{\alpha\beta}(R)=\frac{Z_\alpha Z_\beta}{R}+\tilde{\phi}_{\alpha\beta}(R)\ . \quad (22)$$

In Eq. (22) Z_α and Z_β denote the ionic charges, and the long-range Coulomb part has been separated from the short-range contribution $\tilde{\phi}_{\alpha\beta}$. The latter is given by

$$\tilde{\phi}_{\alpha\beta}(R)=z_\alpha U_\beta(R)+z_\beta U_\alpha(R)+W_{\alpha\beta}(R)+G_{\alpha\beta}(R)\ , \quad (23)$$

with

$$U_\alpha(R)=\int dV\rho_\alpha(\mathbf{r})\left[\frac{1}{R}-\frac{1}{|\mathbf{R}-\mathbf{r}|}\right] \quad (24)$$

and

$$W_{\alpha\beta}(R)=\int dV\,dV'\rho_\alpha(\mathbf{r})\rho_\beta(\mathbf{r}')\left[\frac{1}{|\mathbf{r}-\mathbf{r}'-\mathbf{R}|}-\frac{1}{R}\right] \quad (25)$$

and

$$\begin{aligned}G_{\alpha\beta}(R)=\int dV\{&[\rho_\alpha(\mathbf{r})+\rho_\beta(\mathbf{r}-\mathbf{R})]\\&\times\epsilon[\rho_\alpha(\mathbf{r})+\rho_\beta(\mathbf{r}-\mathbf{R})]-\rho_\alpha(\mathbf{r})\epsilon[\rho_\alpha(\mathbf{r})]\\&-\rho_\beta(\mathbf{r}-\mathbf{R})\epsilon[\rho_\beta(\mathbf{r}-\mathbf{R})]\}\ .\end{aligned} \quad (26)$$

z_α and z_β are the nuclear charges of the interacting ions and ϵ in Eq. (26) is given by the LDA expression for the energy treating the kinetic energy in the Thomas-Fermi approximation,

$$\epsilon(\rho)=\epsilon_k(\rho)+\epsilon_x(\rho)+\epsilon_c(\rho)\ , \quad (27)$$

where

$$\epsilon_k(\rho)=\tfrac{3}{10}(3\pi^2\rho)^{2/3} \quad (28)$$

and

$$\epsilon_x=-\frac{3}{4}\left[\frac{3\rho}{\pi}\right]^{1/3}\ , \quad (29)$$

while the correlation energy per electron ϵ_c is taken according to Ref. 12.

The $\tilde{\phi}_{\alpha\beta}(R)$ are calculated numerically for different values of the distance R between the ions and the results are fitted to the following two-exponential form:

$$\tilde{\phi}(R)=\alpha_+e^{-\beta_+R}-\alpha_-e^{-\beta_-R}\ , \quad (30)$$

which is suggested by Eqs. (23)–(26) and which deviates from the Born-Mayer form of the pair potentials frequently utilized in empirical calculations. The force constants of our ionic model then are obtained by differentiating $\phi_{\alpha\beta}$ twice with respect to the ion coordinates and the dynamical matrix of the reference system is determined in the usual way from the force constants by a Fourier transformation. Finally, the energy of the ionic system

$$E=\frac{1}{2}\sum_{\mathrm{b},\alpha,\beta}{}'\,\phi_{\alpha\beta}(|\mathbf{R}_\beta^{\mathrm{b}}-\mathbf{R}_\alpha^0|) \tag{31}$$

is minimized with respect to the four structure parameters a (lattice constant), c/a (ratio of c axis to lattice constant), $z(\mathrm{La}),z(\mathrm{O}_z)$ (positions of La and O_z in the elementary cell).

B. Structure parameters and dispersion in the ionic model

The results from the minimization of the energy of the ionic system are collected in the first row of Table I and are compared with the results of the so-called potential-induced breathing model[15] (PIB) and the experimental values.[16] The PIB model is like ours, an *ab initio* ionic model where the charge density in the crystal is also given by overlapping Watson-sphere stabilized ions. In contrast to our model, the ionic densities in the PIB model are assumed to depend on the actual configuration of the ions via the Madelung potential, such that the radius of the Watson sphere varies dynamically with the Madelung potential when the ions are vibrating.

From the data in Table I we find that there are only small differences between the results of the PIB model and our rigid-ion model (RIM) as far as the structure parameters are concerned. Compared to the experiments, both models lead to an enhanced planar lattice constant and to a (c/a) ratio, which is too small. This can be considered to be a consequence of the use of spherical ions overestimating the repulsion between the Cu and $\mathrm{O}_{x,y}$ ions in the plane. Note, however, that the model gives (in spite of the overestimate of the in-plane lattice parameter) a large part of the elongation of the CuO_6 octahedron, being related in this way to the layered tetragonal structure and the strong ionic forces. The remaining part of the elongation then arises from the nonspherical shape of the ions not taken into account. Indeed, complete LDA calculations lead to a better agreement with the experimental structural parameters[2] and one may be tempted to reduce the long-range Coulomb interaction simply by taking some effective ionic charges (e.g., from LDA calculations) instead of the completely ionized picture. We have performed such a replacement of the charges in a calculation of the phonon dispersion leading, however, to a larger number of unstable branches as compared with the calculation using the nominal charges. On the other hand, the high-frequency optical branches are not softened significantly.

TABLE I. Structure parameters for the minimum of energy of the ionic reference model (first row). Comparison is performed with the PIB model (Ref. 15) and the experimental results (Ref. 16).

	a (Å)	c/a	z (O_z)	z (La)
	3.98	3.02	0.190	0.363
PIB	4.06	3.01	0.193	0.366
Expt.	3.79	3.49	0.182	0.362

In Fig. 1 the phonon-dispersion curves of our ionic reference model for the tetragonal phase of La_2CuO_4 are displayed for the $\Delta\sim(1,0,0)$, $\Lambda\sim(0,0,1)$ and $\Sigma\sim(1,1,0)$ direction. Compared with the results of the PIB model[15] we find good agreement in the Σ direction. In the other directions no PIB results are published. Thus we conclude that spherical "breathing corrections" to the ionic charge densities, which are additionally considered in the PIB model, are not very essential for the phonon dispersion in La_2CuO_4. The occurrence of imaginary frequencies in the PIB model and also in the RIM developed in this paper cannot be considered as a drawback. Instead it may be regarded as a reflection of real physical properties of the system, like instabilities or anharmonicities related to the ionic character of the forces.[2,3,15] For example, the lowest frequency at the X point corresponds to a rotation of the octahedra around the z axis that hardly can be stabilized in the model. The next most unstable mode at X is the tilt mode and the instability of this mode announces correctly the phase transition from the tetrago-

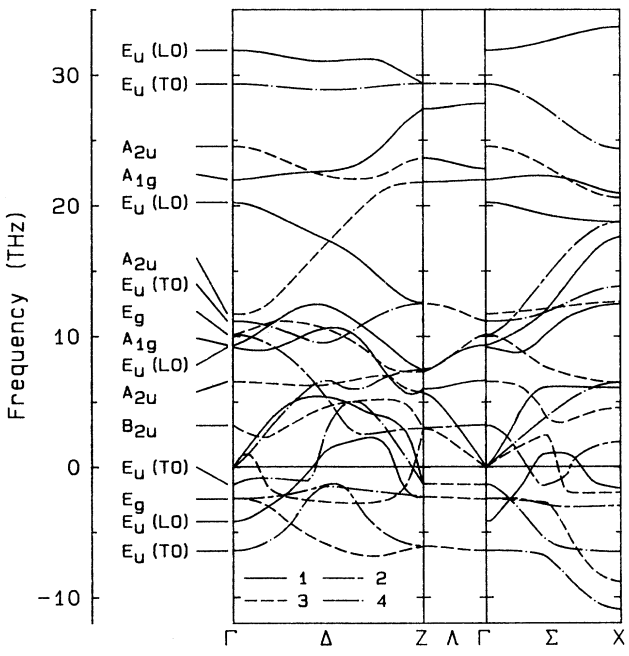

FIG. 1. Calculated phonon dispersion of La_2CuO_4 for the ionic reference model in the main symmetry directions $\Delta\sim(1,0,0)$, $\Lambda\sim(0,0,1)$, and $\Sigma\sim(1,1,0)$. The classification of the phonon branches by irreducible representations (with symmetry labels 1–4) has been brought about in the figure by using different line types. Imaginary frequencies are represented as negative numbers. Note that the numbering of the irreducible representations 3 and 4 in Δ and Σ directions is reversed as compared to the convention in Refs. 18–21.

nal to the orthorhombic structure observed experimentally. The lowest frequency at the Γ point is connected with a sliding motion of the O_z ions parallel to the plane and the unstable E_g mode involves sliding of both O_z and La ions. These results point in the direction of large amplitude motion of these ions and towards possible anharmonicities. Another interesting feature of the dispersion is the LO-TO splitting of the E_u modes and the discontinuity of the A_{2u} vibrations at the Γ point. The E_u vibrations are polarized in the xy plane and are twofold degenerate while the A_{2u} vibrations are polarized along the z axis and are nondegenerate. The splitting of the E_u vibration with the highest and lowest frequency is relatively small while the splitting of the two other optical E_u modes is large. The largest splitting (discontinuity) of all modes is found for the A_{2u} mode with highest frequency. Practically no splitting is present for the lowest optical A_{2u} mode, which means that the dipole moment of the elementary cell is approximately zero because of the specific ratio of the amplitudes of vibration of the different sublattices.

Of particular interest is the so-called planar oxygen breathing mode at the X point where the four $O_{x,y}$ ions (and to some extent the two O_z ions) are vibrating against the central Cu ion. Because of the in-phase movement and the correspondingly large variation of the Cu-O bond length for this vibration, a strong renormalization of the frequency is to be expected when applying the ideas of a standard screening approach for high-density metals. Indeed, in such a description of lattice dynamics,[17] which works well for good metals but ignores the effects of long-range ionic forces emphasized in this work, leads to a strong decrease in frequency in the doped material and even to an instability in the undoped case. However, from experiments[18–21] and also in our ionic model, the planar oxygen breathing mode is the hardest mode, rather than being the softest as in Ref. 17.

A global comparison of the results for the phonon dispersion as calculated from the ionic model (or the PIB model) with the (still incomplete) experimental curves shows that the former are about 30% too high. But one should remember that contributions to the density response, which can be ascribed to covalent and metallic effects of the system, have been neglected. Nevertheless, important qualitative features of the ionic model dispersion also can be found in the experimental results. For example, there is an increasing Σ_1 phonon branch with the highest frequencies of the spectrum when going from the Γ point to the X point, ending at the planar oxygen breathing mode. Also the proportions of the LO-TO splittings agree in experiment and calculation. The splitting of the highest E_u mode is small in the calculation and not seen at all in experiment. There are two large LO-TO splittings in the intermediate range of frequencies and a large discontinuity of the A_{2u} mode ("ferroelectric mode") in theory as well as in experiment. The lowest E_u mode splitting is small both in theory and experiment. Furthermore, we extract from the experimental results[20,21] that in the doped (metallic) phase of La_2CuO_4, the LO-TO splittings and the large A_{2u} discontinuity vanish. The latter fact indicates a metallic screening also in the z direction. In connection with the vanishing of the A_{2u} discontinuity, there appears a characteristic Λ_1 phonon branch with a very steep dispersion. Of course, these features cannot be explained in an ionic model and an explanation will be provided by considering charge fluctuations as the dominating screening mechanism.

Another interesting feature of the experimental dispersion is the anomalous softening of the highest Δ_1 branch midway in the Δ direction. Comparing the results for the metallic phase with the insulating phase, this minimum in the dispersion curve is deepened significantly.[20,21] In outlines, this minimum is already present in the corresponding dispersion curve of the ionic model (see Fig. 1). The displacement pattern of the ions in this mode is similar to the planar breathing mode. But only one pair of oxygen ions (O_x) in the plane is vibrating against the Cu ion while the other pair is silent. In view of the similarity of the displacement patterns of both modes it looks strange that the highest Σ_1 branch does not show any anomalous softening, not even in the metallic phase. A possible explanation of such behavior is presented below, taking charge-fluctuation effects at the Cu and $O_{x,y}$ ions into account.

Another interesting feature of the phonon dispersion in the ionic model (and also in the insulating model, see below) should be mentioned, namely, that the axial O_z breathing mode (O_z^z) is the highest Λ_1 mode at the Z point [compare with Fig. 1 and 3(b)]. This fact was not recognized in the experimental work published so far. However, very recently we became aware of new experimental results[22] where O_z^z has been found as the highest Λ_1 mode at the Z point. This phonon is unusually broad and therefore it was not detected in earlier measurements. We think that nonlocal electron-phonon interaction effects of charge-fluctuation type are very significant especially for this mode.[23] Our calculations of the long-range changes of the effective (screened) potential in the CuO plane accompanying this mode give particularly large values in the model for the insulating phase. A discussion of the importance of this phonon for an understanding of a nonconventional phonon-mediated pairing mechanism in the HTSC, based on long-range electron-phonon interaction effects, can be found in Ref. 23, using the method presented in Sec. II and will be reviewed later on in this work.

C. Implementation of the charge-fluctuation degrees of freedom

Next we sketch the way we have implemented approximatively the EDF of the charge-fluctuation type, simulating the screening effect in the HTSC. According to the formalism developed in Sec. II, we have to calculate the interaction of the charge-fluctuation degrees of freedom (CFDF) with the ions ($B^{b\kappa A}_i$) and the mutual interaction of the CFDF ($C^{ab}_{\kappa\kappa'}$). In doing so, we have to observe that the formalism presented in Sec. II is developed for a situation where the change in density $\mathbf{P}^{\mathbf{A}}$ is fully described by

the EDF according to the minimum principle for the energy. However, in our present model the main part of $\mathbf{P}^{\mathbf{A}}$ is given explicitly by the movement of the rigid ions (see the remark at the beginning of Sec. III A). The quantity $B^{\mathbf{b}\kappa\mathbf{A}}_{i}$ then contains, besides the coupling of ρ_κ with the potential of the ion core, as it is expressed by Eq. (17), an additional contribution caused by the interaction between ρ_κ and the ionic densities ρ_α via F''.

The important long-range Coulomb contributions can be separated, i.e.,

$$[B^{\mathbf{b}\kappa\mathbf{A}}_{i}]_c=\frac{\partial}{\partial R_i^{\mathbf{A}}}\left[\frac{Z_\alpha}{|\mathbf{R}^{\mathbf{A}}-\mathbf{R}^{\mathbf{b}}_{\kappa}|}\right], \tag{32}$$

$$[C^{\mathbf{ab}}_{\kappa\kappa'}]_c=\frac{1}{|\mathbf{R}^{\mathbf{b}}_{\kappa'}-\mathbf{R}^{\mathbf{a}}_{\kappa}|}, \tag{33}$$

and can be dealt with exactly using the Ewald method. In order to estimate the short-range part of $B^{\mathbf{b}\kappa\mathbf{A}}_{i}$ we identify the form factors ρ_κ with the Cu-d and O-p orbital densities, respectively, and confine ourselves to the Hartree contribution in F''. The ionic densities ρ_α are already known from the ionic model and the form factors ρ_κ are calculated with our modified Herman-Skillman program. In this way we get at least an idea of the order of magnitude of the short-range contribution to $B^{\mathbf{b}\kappa\mathbf{A}}_{i}$.

The mutual interaction of the CFDF $C^{\mathbf{ab}}_{\kappa\kappa'}$ according to Eqs. (12) and (13) contains contributions from the Coulomb- and exchange-correlation interaction as well as a contribution from the kinetic energy. The long-range Coulomb part is given in Eq. (33) and the short-range Coulomb part can be estimated in a similar way as in the case of $B^{\mathbf{b}\kappa\mathbf{A}}_{i}$, approximating the form factors ρ_κ and $\rho_{\kappa'}$ by the Cu-d and O-p orbital densities.

Most important are the self-interaction terms $\tilde{V}^{\mathbf{aa}}_{\kappa\kappa'}$. They represent the change in Coulomb- and exchange-correlation energy, which is connected with the charge fluctuation on a certain ion. Small values of these quantities mean that it is easy to excite charge fluctuations at the corresponding ion, while large values tend to suppress such fluctuations. The mutual interplay of the self- and interaction terms and their interplay with contributions from the kinetic energy via the polarizability π in Eq. (14) is very significant for our model and reflects the relative importance of localization and delocalization properties of the electrons in the crystal. Such features are strongly related to electronic correlation effects, e.g., a large Cu self-term on the one hand, and to specific characteristics of the Fermi surface and band structure, e.g., nesting features on the other hand.

Before discussing the approximate calculation of the kinetic contribution in terms of the polarizability $\pi^{\mathbf{ab}}_{\kappa\kappa'}$, we would like to remark that the approach in Sec. II also allows us to apply a semiempirical model concept by parametrizing the short-range parts of $B^{\mathbf{b}\kappa\mathbf{A}}_{i}$ and $C^{\mathbf{ab}}_{\kappa\kappa'}$ (i.e., the strong local correlations), in contrast to the parameter-free approach we have outlined so far. Such a strategy is also useful because strong local correlations are very hard to compute in a realistic way and so microscopic model calculations of specific effects (like characteristics in the dispersion) can help identify the relevant quantities which reflect the correlations.

From its definition $(-\pi^{\mathbf{ab}}_{\kappa\kappa'})$ means the change $\delta\zeta^{\mathbf{a}}_{\kappa}$ of the EDF $\zeta^{\mathbf{a}}_{\kappa}$ in response to a variation of the total self-consistent potential at the position of the EDF $\zeta^{\mathbf{b}}_{\kappa'}$. For the calculation of $\pi^{\mathbf{ab}}_{\kappa\kappa'}$ we use the tight-binding (or Wannier) representation for the polarizability,[6]

$$\pi(\mathbf{q}+\mathbf{G},\ \mathbf{q}+\mathbf{G}')=\sum_{s,s'} A_s(\mathbf{q}+\mathbf{G})e^{-i\mathbf{G}\cdot\mathbf{R}^{\mu}}\pi_{ss'}(\mathbf{q})A^{*}_{s'}(\mathbf{q}+\mathbf{G}')e^{i\mathbf{G}'\cdot\mathbf{R}^{\mu'}}, \tag{34}$$

with

$$A_s(\mathbf{r})\equiv\varphi^{*}_{\mu}(\mathbf{r})\varphi_{\nu}(\mathbf{r}-\mathbf{R}^{s}),\quad s=(\mu\nu\mathbf{a}),\mathbf{R}^{s}=\mathbf{R}^{\mathbf{a}}_{\nu}-\mathbf{R}^{\mu}, \tag{35}$$

as overlap densities of the tight-binding (Wannier) functions and

$$\pi_{ss'}(\mathbf{q})=-\frac{2}{N}\sum_{n,n',\mathbf{k}}\frac{f_n(\mathbf{k})-f_{n'}(\mathbf{k}+\mathbf{q})}{\epsilon_n(\mathbf{k})-\epsilon_{n'}(\mathbf{k}+\mathbf{q})}[C^{*}_{\mu n}(\mathbf{k})C_{\nu n'}(\mathbf{k}+\mathbf{q})][C^{*}_{\mu' n}(\mathbf{k})C_{\nu' n'}(\mathbf{k}+\mathbf{q})]^{*}e^{i(\mathbf{k}+\mathbf{q})(\mathbf{R}^{s}-\mathbf{R}^{s'})}. \tag{36}$$

The f's, ϵ's, and C's represent the occupation numbers, the electronic bandstructure, and the expansion coefficients of the Bloch functions in terms of tight-binding (Wannier) functions. The CFDF are described by a submatrix of $\pi_{ss'}$ with $\mu=\nu\equiv\kappa$, $\mathbf{a}=\mathbf{0}$, and $\mu'=\nu'\equiv\kappa',\mathbf{b}=\mathbf{0}$, which then defines the Fourier transform $\pi_{\kappa\kappa'}(\mathbf{q})$ of $\pi^{\mathbf{ab}}_{\kappa\kappa'}$. Here the form factors have been identified with the self-overlap densities $A_{\mu\mu 0}(\mathbf{r})$.

For the calculation of $\pi_{\kappa\kappa'}(\mathbf{q})$ we use a two-dimensional tight-binding model for the band structure,[24] which is in qualitative agreement with the full three-dimensional results.[2,25] The basis set of this model consists of five 3d orbitals on the copper and three 3p orbitals on each of the two oxygens (eleven-band model). In the π matrix we allow for charge fluctuations on the Cu and $O_{x,y}$ and only the Cu $d_{x^2-y^2}$ and the O_x, O_y p orbital pointing towards the Cu are taken into account, yielding a 3×3 matrix.

Figure 2 shows our results for $\pi_{\kappa\kappa'}(\mathbf{q})$ in the main symmetry directions in the two-dimensional Brillouin zone for the undoped [Fig. 2(a)] and doped case [Fig. 2(b)], respectively. In the undoped case we get a nesting peak at the M point of the two-dimensional zone (X point of the three-dimensional zone). See also the calculations reported for the susceptibility in Ref. 2, yielding similar results.

Generally, nesting properties of the Fermi surface are reflected by peaks of the polarizability at the corresponding nesting vectors. This can lead, if strong enough, to either a charge density wave (CDW) or a spin density wave (SDW), or to both.

The tendency for the development of an electronic superstructure by a CDW transition (possibly accompanied by a lattice soft mode in the system) occurs if, in addition to the effect introduced through the nesting behavior in π, we have a small or negative $\tilde{V}(\mathbf{q})$ in Eq. (14). This can only happen if the self-interaction terms $\tilde{V}^{aa}_{\kappa\kappa}$ are not too large. On the other hand, we know that a CDW transition is absent in La_2CuO_4 (and the other copper-oxide superconductors) indicating that the copper self-interaction is still large, even in the metallic phase. This fact will prove to be important for the understanding of special features of the phonon dispersion to be discussed below. In context with a large copper self-interaction, it is further interesting to note that the isotope exponent α, being very small in the HTSC, is rather dependent on the nature of the interactions among the electrons. For example, following the treatment of the isotope effect as presented in Ref. 26, we find that small values for α correlate with large values of the intra-atomic Coulomb repulsion. Both the dependence of α on the electronic structure (density of states, correlation) and the anharmonicity of certain phonon modes (see our findings in the ionic model) will play a role for the anomalous behavior of the isotope effect in the HTSC.

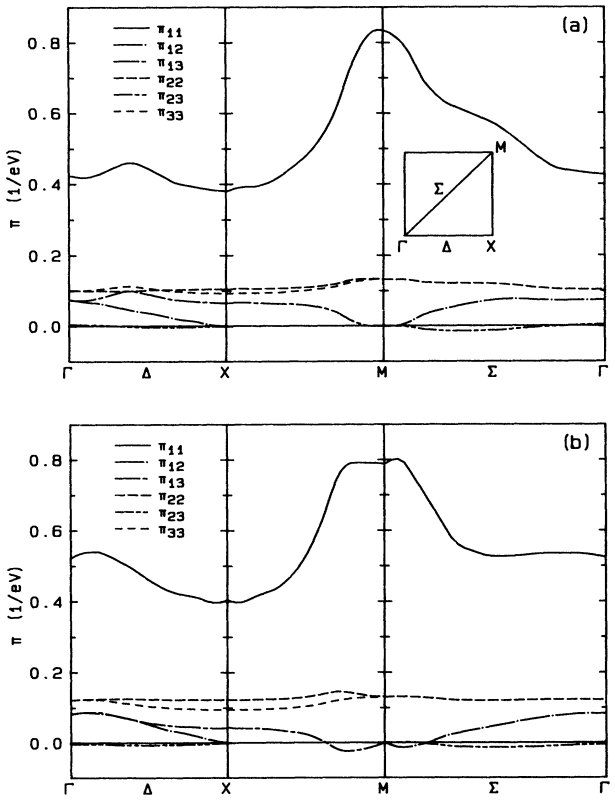

FIG. 2. Dispersion of the matrix elements $\pi_{\kappa\kappa'}(\mathbf{q})$ of the polarizability according to Eq. (36) using the two-dimensional tight-binding model for the band structure as explained in the text. Figures 2(a) and 2(b) display the results for the undoped and doped case, respectively. The different elements $\pi_{\kappa\kappa'}$ are represented by different line types. The two-dimensional Brillouin zone is shown as an inset.

The position of the peak at $M(X)$ is significant because it coincides with the ordering wave vector of the antiferromagnetic state. In the doped case [Fig. 2(b)] the peak in the polarizability in shifted to a smaller wave vector. In both cases the dominant contribution to π arises from the diagonal Cu-Cu polarizability (π_{11} in Fig. 2) for which we recognize the nesting peak at $M(X)$ in the undoped material, being shifted inward in the doped case. The diagonal O-O polarizabilities [π_{22} (O_x) and π_{33} (O_y)] are significantly smaller than π_{11} and do not show noticeable nesting behavior. Next in magnitude are the off-diagonal Cu-O polarizabilities π_{12} and π_{13}. The off-diagonal O-O polarizability π_{23} is practically zero. If the Cu-O polarizability is large enough, it can reverse in certain phonon modes the direction of the charge transfer as compared with a situation where the diagonal polarizability dominates. For example, this can be achieved for the axial oxygen breathing mode at the Γ point (O_z^{Γ}) by arbitrarily increasing π_{12} and π_{13} in our model. Compare this with the findings in Refs. 2, 15, where for this mode such a counter intuitive shift of charge between the Cu and the in-plane $O_{x,y}$ is reported. For the O_z^z mode in the metallic phase, our calculations show no reversal in sign for the charge transfer upon increasing π_{12} and π_{13}, but a strong increase of the charge fluctuations on the Cu ions at the cost of the charge fluctuations on $O_{x,y}$.

In the case of the doped material, the Fermi energy coincides with a Van-Hove singularity, leading to an increase of the density of states at E_F. This fact is reflected by the increase of the polarizability at the Γ point [see Fig. 2(b)]. From the band-structure model used for the calculation of π, we cannot expect to obtain "high quality" results for the polarizability. Our main concern is to get an idea of the absolute and relative order of magnitude of the individual matrix elements, including their dispersion as a function of the wave vector $\mathbf{q}$. So, for the practical use of π in Eq. (14), we parametrize our numerical results by a low-order Fourier decomposition.

An important question remains as to how to discriminate between the density response of a metal and that of an insulator. A general criterion follows from the different analytical behavior of the Fourier-transformed polarizability matrix $\pi(\mathbf{q}+\mathbf{G},\mathbf{q}+\mathbf{G}')$ in the long-wavelength limit ($\mathbf{q}\rightarrow\mathbf{0}$) in both phases.[27,28] We can adapt this criterion to the formulation of the density response as presented in Sec. II and find

$$\sum_{\kappa\kappa'}\pi_{\kappa\kappa'}(\mathbf{q}\rightarrow\mathbf{0})=\begin{cases}O(q^2) & \text{insulator}\\ Z(E_F) & \text{metal}\end{cases} \tag{37}$$

and

$$\sum_{\kappa'}\pi_{\kappa\kappa'}(\mathbf{q}\rightarrow\mathbf{0})=O(q) \quad \text{insulator.} \tag{38}$$

The expression in Eq. (38) is different from zero in the long-wavelength limit in the case of a metal. $Z(E_F)$ in

Eq. (37) means the density of states at the Fermi level. The left-hand side of Eq. (37) is proportional to the compressibility κ_T of the electronic system. The latter provides a quantitative measure of the gap in the electronic spectrum because κ_T vanishes as a function of the chemical potential in the gap region. It is just this relation which is expressed by Eq. (37) in the case of an insulator. This equation can be considered as a closed form to characterize the metal-insulator transition and we see that such a transition occurs at a density as the controlling quantity where the static and long-wavelength limit of the polarizability vanishes. We further realize that in the insulating phase the charge fluctuations are strongly restricted by Eqs. (37) and (38), in the course of which the incompressibility related to the gap in the energy spectrum of the system leads to a strong suppression of long-wavelength density fluctuations. In the case of a metal with no gap in the spectrum, the fluctuations are less restricted. In particular, Eq. (38) does not hold, and long-wavelength fluctuations become possible, and the compressibility in the metallic phase of the HTSC can be thought to be induced by ionic charge fluctuations in our model.

D. Phonon dispersion including charge fluctuations

We now discuss our results on the influence of the CFDF on the phonon dispersion. We first consider the doped (metallic) phase of La_2CuO_4 in Fig. 3(a). The dispersion curves for the undoped (fictitious insulating) phase displayed in Fig. 3(b) are obtained by requiring the matrix elements of $\pi_{\kappa\kappa'}(\mathbf{q})$ to fulfill the density-response conditions provided by Eqs. (37) and (38) for an insulator.

We begin with the highest frequency vibrations which are the oxygen vibrations in the CuO plane. In accordance with experiment, the highest Δ_1 branch is decreased below Δ_4 and now shows the characteristic dip of the experimental dispersion midway in the Δ direction. Also, the highest Σ_1 branch is decreased relative to the ionic model but still shows the correct increasing dispersion towards the X point. In order to get a better understanding of the behavior of these phonon branches, we have performed calculations suppressing either the charge fluctuations at the copper or at the oxygen, respectively, by choosing arbitrarily large values for the corresponding self-interaction terms $\tilde{V}^{aa}_{\kappa\kappa}$ (U_d for Cu and U_p for O). The results for the phonon dispersion [Figs. 4(a) and 4(b)] demonstrate the dominant influence of the Cu charge fluctuations as far as the highest Δ_1 and Σ_1 branches are concerned. For the X-point breathing mode, for example, by increasing U_d the charge fluctuations $\delta\zeta$ [Eq. (21)] at the Cu are strongly suppressed and the frequency is raised. There are no charge fluctuations $\delta\zeta$ at $O_{x,y}$ in this mode for symmetry reasons [see also Fig. 4(b)]. This is quite in contrast with the situation at the Δ_1 minimum. Here, beside the charge fluctuation at the Cu responsible for the main part of the minimum [(Fig. 4(a)], we have additional charge fluctuations at the nonvibrating O_y ions [Fig. 4(b)], further softening this mode.

To get the results displayed in Fig. 5, we have investigated the combined effect of the short-range part of the force on the CFDF at the Cu ion if the O_x or O_y ion is displaced (B_1), and of the self-interaction term U_d at the Cu on the dispersion of the highest Δ_1 and Σ_1 branch. The results might help one to understand the experimental fact that in doped La_2CuO_4 there is a pronounced softening of the highest Δ_1 branch midway in the Δ direc-

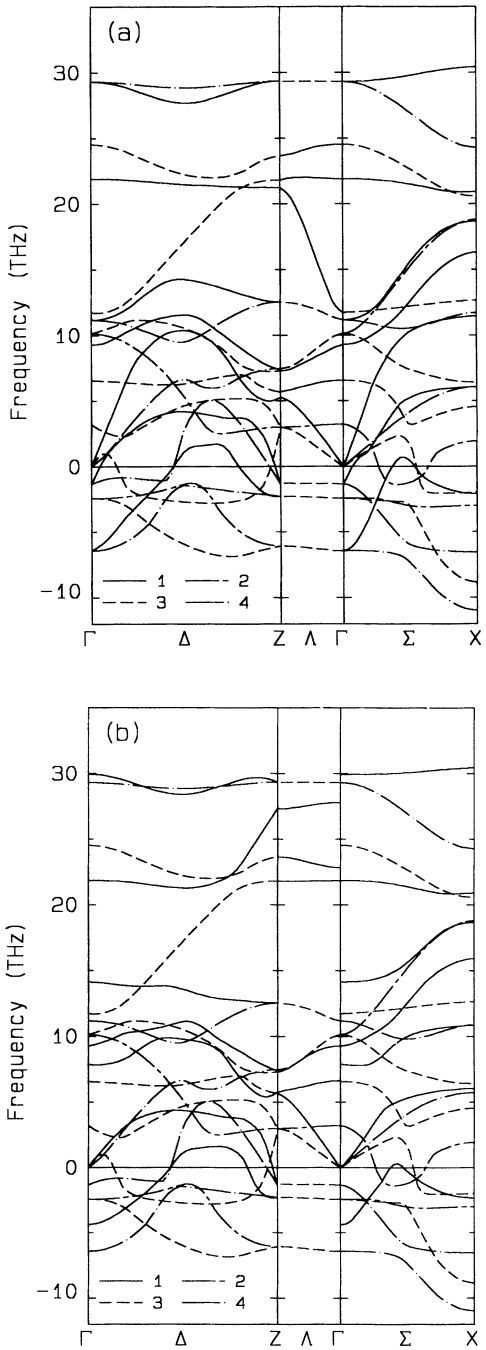

FIG. 3. Phonon dispersion of La_2CuO_4 taking charge fluctuations at the copper and oxygen in the plane into account. (a) gives the results for the metallic phase and (b) for the insulating phase. The labeling of the curves is the same as in Fig. 1.

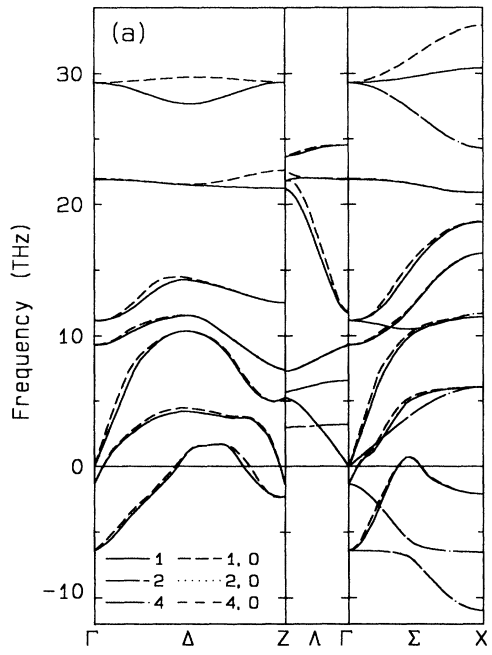

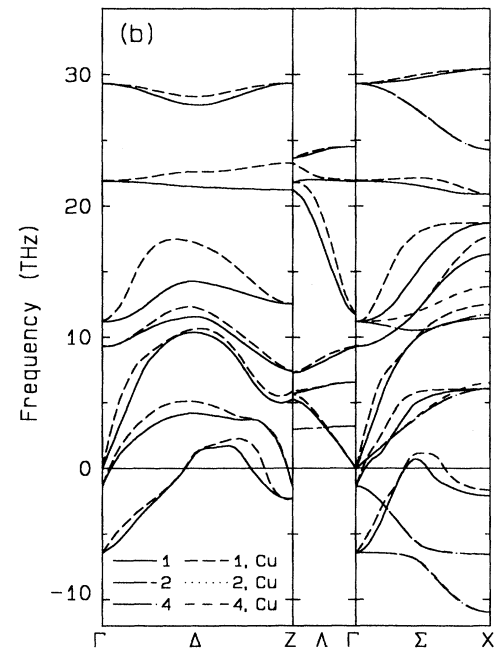

FIG. 4. Phonon dispersion of metallic La_2CuO_4 (a) suppressing the charge fluctuations at the Cu (only oxygen charge fluctuations are allowed) and (b) suppressing the fluctuations at $O_{x,y}$ (only copper charge fluctuations are allowed). For comparison, the results of the full calculation (linetypes ——1, ——−2, ——·4) are also shown. Only the branches of symmetries allowing for charge fluctuations are shown.

tion.[20,21] The tendency for such a behavior can already be seen in Figs. 3(a) and 3(b). Physically we expect that the charge fluctuations at the Cu and the corresponding decrease in frequency are larger, the smaller U_d happens to be. The results of Fig. 5 confirm this expectation. A negative value for B_1 weakens the charge transfer at the Cu and thus increases the phonon frequency. Ignoring B_1 and choosing a small enough value for U_d increases the charge fluctuations at the Cu and a decreasing dispersion of Σ_1 towards the X point can result (see the broken curve in Fig. 5). This contradicts experimental evidence but points toward the direction of the "expected" result in a normal high-density metal.[17] It can be expected that the self-interaction U_d changes with increasing bandwidth from a site-classified Coulomb interaction to a screened Coulomb interaction at high doping. From our discussion above, it is clear that reducing the self-interaction U_p will also soften the Δ_1 minimum because of the enhancement of the charge fluctuation at O_y, without increasing the frequency of the planar-breathing mode. This is confirmed by the numerical results displayed in the dotted curve of Fig. 5.

The second highest Δ_1 branch with O_z^z as its endpoint and the Λ_1 branch with the steep dispersion are influenced by charge fluctuations at both the Cu and $O_{x,y}$ (Fig. 4), leading to an effective screening of the long-range Coulomb interactions which are responsible for the high frequencies of O_z^z and the highest Λ_1 branch in the ionic and insulating model [Figs. 1 and 3(b)]. The intermediate and lower lying branches are dominated by oxygen charge-transfer effects.

Compared with the ionic model from Fig. 1, there is

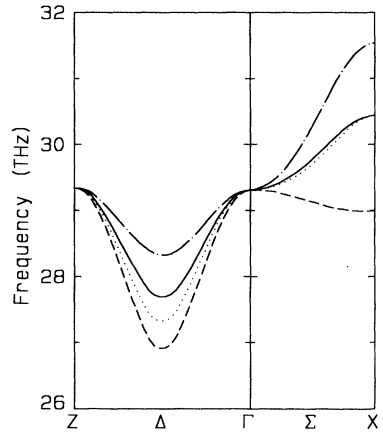

FIG. 5. Dispersion of the highest Δ_1 and Σ_1 branch in the metallic phase of La_2CuO_4 for different choices of the self-interaction terms at the Cu (U_d) and at $O_{x,y}$ (U_p) as well as for different values of the short-range part of the force on the CFDF at the Cu if O_x or O_y is displaced (B_1). The different sets of parameters (U_d, U_p, B_1) are characterized by different linetypes: ——· ($U_d=7.6$, $U_p=3.4$, $B_1=-3.9$), —— ($U_d=5.5$, $U_p=3.4$, $B_1=-3.9$, this set was used to obtain the results displayed in Fig. 3), · · · ($U_d=5.5$, $U_p=1.7$, $B_1=-3.9$), — — — ($U_d=5.5$, $U_p=3.4$, $B_1=0$). U is in units of (e^2/a) and B_1 in e^2/a^3. e = elementary charge and a = lattice constant.

further a drastic rearrangement of the phonon dispersion in the metallic phase when charge fluctuations are taken into account [see Figs. 1, 3(a), and 6(a)]. The LO-TO splittings of the E_u modes and the large A_{2u} discontinuity at the Γ point are vanishing as a consequence of the metallic charge transfer. In connection with the removal of the A_{2u} discontinuity, we observe a large decrease of the second highest Δ_1 branch, especially at the Z point, and of the highest Λ_1 branch. (A detailed discussion of the charge fluctuations in O_z^z will be given later, see also Table II). This results in the Λ_1 branch with the steep dispersion, which quite recently[20,21] also has been observed in doped La_2CuO_4. The very drastic renormalization of the third highest and third lowest Δ_1 and Σ_1 branches is caused by the vanishing of the LO-TO splittings. So we have metallic behavior in the plane where the E_u modes are polarized, as well as in the z direction, the polarization direction of the A_{2u} modes.

Looking a bit closer at the phonon dispersion of the insulator [Figs. 3(b) and 6(b)], we find that the LO-TO splittings are reduced in comparison with the ionic reference model because charge fluctuations are now possible, however, under the restricting conditions from Eqs. (37) and (38). On the other hand, the discontinuities of the A_{2u} modes at Γ do not change at all and the highest Λ_1 branch, including O_z^z, remains practically unchanged from the ionic model. The reason for this behavior is because of the assumption of two-dimensional electronic structure in our model. This confines, in the case of an insulator, the charge fluctuations locally within the CuO planes in contrast to the metallic phase where interplane charge transfer is possible even if the electronic structure is two dimensional. These interplane processes lead, in the metallic phase, to the large renormalization of O_z^z, the highest Λ_1 branch, and to the vanishing of the A_{2u} discontinuity. See also the discussion below and note that a macroscopic electric field in the z direction which accompanies the longitudinal A_{2u} vibration cannot be screened by local charge rearrangements within the planes.

A noticeable renormalization of O_z^z and of the highest Λ_1 branch in the insulating phase can, however, be achieved by installing charge-fluctuation centers at O_z (see Fig. 7), thereby giving up the strictly two-dimensional electronic structure. Inspection of the behavior of these phonon modes can give some insight concerning the importance of the "third dimension" of the electronic structure in the HTSC. Indeed, recent self-interaction corrected local spin-density calculations for La_2CuO_4 (Ref. 29), which are in agreement with the experimentally observed antiferromagnetic and insulating ground state, suggest that all oxygen degrees of freedom should be incorporated in model studies of superconductivity.

E. Charge fluctuations in the axial breathing modes

In the final part of this paper we discuss the relevance of nonlocal electron-phonon interaction effects of charge-fluctuation type for the axial O_z- and La_z-breathing modes at the Γ and Z point ($O_z^\Gamma, O_z^z, La_z^\Gamma, La_z^z$) and demonstrate how the usual picture of electron pairing has to be modified by including these nonlocal effects. Both O_z modes are symmetric breathing vibrations along the z axis; however, in O_z^z, the O_z ion pairs are vibrating in opposite directions in consecutive layers while in O_z^Γ the vibration pattern of the O_z pairs is the same in all layers.

From the general expressions of the electron-phonon matrix elements given in Eqs. (18)–(21) we find that the charge fluctuations in a certain phonon mode $\delta\zeta_\kappa^{(q\sigma)}$ provide the screening of the changes in the ion potential in our model.

Within this screening mechanism, long-range (Madelung-like) changes of the effective potential will survive, even in the metallic phase, when certain ions are displaced. The discussion above has shown that these changes are very important for an understanding of the phonon dispersion. On the other hand, such effects are ignored in the standard theory of electron-phonon interaction based on the rigid-ion or muffin-tin approxima-

TABLE II. Results for the charge fluctuations $\delta\zeta_\kappa^{(q\sigma)}$, according to Eq. (21), in insulating (first four rows) and metallic (last four rows) La_2CuO_4 for different symmetric axial breathing modes: $O_z^\Gamma, O_z^z, La_z^\Gamma, La_z^z$. ν (in THz) are the corresponding phonon frequencies. e^{O_z} and e^{La} represent the normalized amplitudes of the eigenvectors. $e^{O_z} > 0$ ($e^{La} > 0$) means that O_z(La) is moving away from Cu. The charge fluctuations at the Cu and $O_{x,y}$ are denoted by $\delta\zeta_{Cu}$ and $\delta\zeta_{O_{x,y}}$, respectively. Negative values for $\delta\zeta$ correspond to an increase of electronic charge at the ions.

	ν	e^{O_z}	e^{La}	$\frac{\delta\zeta_{Cu}}{10^2}$	$\frac{\delta\zeta_{O_x}}{10^2}$	$\frac{\delta\zeta_{O_y}}{10^2}$
O_z^Γ	21.85	0.71	−0.02	−0.634	0.317	0.317
O_z^z	27.31	0.67	−0.21	−0.396	0.198	0.198
La_z^Γ	9.26	0.02	0.71	0.400	−0.200	−0.200
La_z^z	5.77	0.21	0.67	−0.792	0.396	0.396
O_z^Γ	21.90	0.71	−0.02	−0.372	0.186	0.186
O_z^z	21.24	0.69	−0.16	−1.696	−1.234	−1.234
La_z^Γ	9.28	0.02	0.71	0.234	−0.117	−0.117
La_z^z	5.29	0.16	0.69	0.105	0.752	0.752

tion, which otherwise constitute the basis for a quantitative description of conventional superconductivity. In these approximations, the picture of the electron pairing mechanism is via a time-retarded interaction between the two electrons (holes) of the pair where the "second" electron (hole) profits from the local change of the potential at the displaced ion previously excited by the "first" electron (hole).

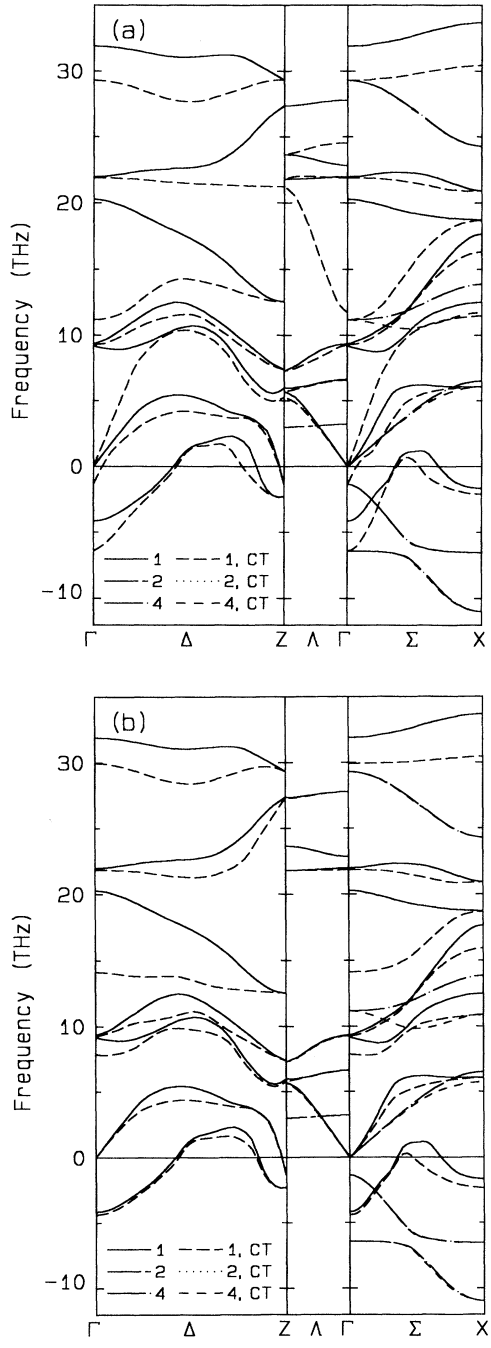

FIG. 6. Phonon dispersion of La_2CuO_4 without (linetypes: —— 1, —— −2, —— ·4) and with charge fluctuations. (a) metallic phase; (b) insulating phase. Only branches for which charge fluctuations are allowed by symmetry are displayed.

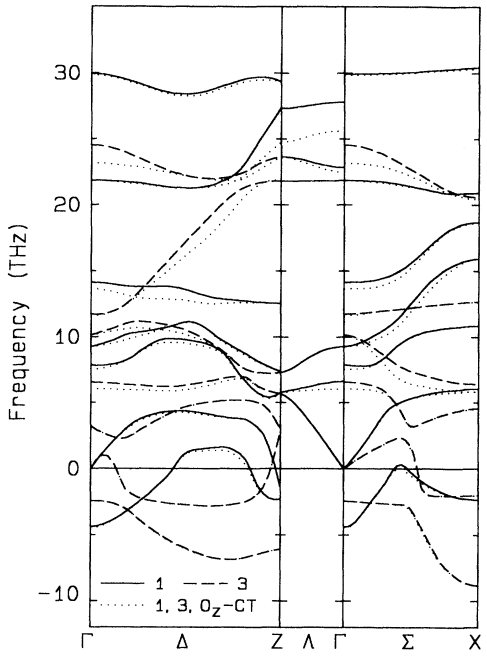

FIG. 7. Phonon dispersion of insulating La_2CuO_4 adding charge-fluctuation centers at O_z. The linetypes ——1, − − −3 represent the case without O_z charge-fluctuation centers and . . . 1,3 represents the results if the latter are considered.

For the following discussion we appeal to the treatment presented in Ref. 23 and recall the "long-wavelength sum rule" from Eq. (38), restricting the density response in an insulator by coupling self-terms and off-diagonal terms in the polarizability of the electronic system. Using Eqs. (14) and (16) in Eq. (21) and observing that for $\mathbf{q}$ parallel to the $\Lambda\sim(0,0,1)$ direction (and in particular at the Z point), we have

$$\pi_{\kappa\kappa'}(\mathbf{q}\|\mathbf{\Lambda})=\pi_{\kappa\kappa'}(\mathbf{q}\rightarrow\mathbf{0}) , \tag{39}$$

if the electronic structure is assumed to be strictly two dimensional (π independent of q_z), we arrive with the help of Eq. (38) at

$$\sum_{\kappa}\delta\zeta_{\kappa}^{(\Lambda\sigma)}=0 \tag{40}$$

for the charge fluctuations in the insulating material. Furthermore, it can be shown that for the Γ-point vibrations considered here we obtain

$$\sum_{\kappa}\delta\zeta_{\kappa}^{(\Gamma\sigma)}=0 \tag{41}$$

for the insulating as well as for the metallic phase. Thus for O_z^z and La_z^z in the insulating phase and O_z^Γ and La_z^Γ in the insulating and the metallic phase, charge transfer is only possible between copper and oxygen ions locally within the plane.

These general results have been confirmed by numerical calculations, which are summarized in Table II. The values for $\delta\zeta_{\kappa}^{(q\sigma)}$ in this table have been obtained with the same model used as a base for the phonon dispersion in this work. They deviate a bit from the values given in

Ref. 23, where the ionic reference system is based on slightly different ionic densities and slightly different numbers have been used for the short-range part of $B^{b\kappa A}_{i}$, $\tilde{V}^{ab}_{\kappa\kappa'}$, and $\pi^{ab}_{\kappa\kappa'}$. (In Table I of Ref. 23 there is a misprint concerning the values of $\delta\zeta$ for the La^z_z vibrations. The correct $\delta\zeta$ values are obtained by correcting for an overall minus sign.)

In the case of the metallic phase, there is no such restricting condition as provided by Eq. (40) for the insulator. As a consequence, in the metal, the O^z_z, and to a lesser extent, the La^z_z vibrations induce fluctuations at the Cu and $O_{x,y}$ that have the same sign in the whole plane (compare with the numerical results in Table II). This finally leads to charge fluctuations of alternating sign in consecutive planes (denoted as "interplane charge transfer") which provide an effective screening mechanism for the long-range Coulomb interactions, being responsible for the high frequency of O^z_z in the insulating and ionic models. Thus, compared with the ionic model [$\nu(O^z_z)=27.37$ THz], we have a strong renormalization of O^z_z in the metal but virtually no decrease in frequency for O^z_z in the insulating model (see Table II) where the interplane charge transfer, characteristic for the screening in the metallic phase, is blocked completely by the strictly two-dimensional electronic structure assumed. This allows for local charge transfer only within the plane and this is less effective for screening. So in this mode the charge fluctuations compensate locally because of the gap in the energy spectrum, while in the metallic phase it becomes favorable to have density changes of the same sign in the whole plane. In the metallic phase the property of an interplane charge transfer as displayed by O^z_z is representative for the whole corresponding Λ_1 branch, however, with decreasing strength when going from Z to Γ, and vanishing at Γ. We would also like to mention that phonons with nonvanishing wave-vector components orthogonal to the Λ direction can generate charge fluctuations of the same sign only along certain directions of the plane.

In context with the strong renormalization of O^z_z in the metallic phase, we obtain an extremely flat dispersion all over along Γ-Δ-Z-Λ-Γ-Σ-X in the frequency range of O^z_z [see Fig. 3(a)]. Such an Einstein mode-like behavior, corresponding to nonpropagating waves at an intermediate optimum phonon region, provides an optimal situation for maximizing T_c in the electron-phonon mechanism.[30]

Ultimately the long-range changes of the effective (screened) potential (accompanying in particular the O^z_z mode), which are possible within the charge-fluctuation-dominated screening mechanism proposed in this paper for the HTSC, but are suppressed by the good metallic screening in the conventional superconductors, can generate an extremely favorable situation for pair binding of electrons (holes). In case the off-diagonal Cu-O polarizability is not too large, which is true for the tight-binding model used here (Fig. 2), we find in the metallic phase of La_2CuO_4 for the O^z_z mode changes of the effective potential having the same sign at all ions in the plane. It is interesting to note that the changes of the potential at the $O_{x,y}$ ions dominate by far the changes at the Cu ions. The following picture for pair binding results: an electron (hole) which comes to pass an ion that previously has been pushed by another electron (hole) does not feel only the local change in potential at the displaced ion (as in the conventional mechanism of pair binding within the RIA), but, additionally, the change in potential of the same sign (mainly at the $O_{x,y}$ ions) in a certain area of the CuO plane. Accordingly, it can lower its energy if the change in potential is attractive during a certain phase of the ionic vibration. For the O^z_z mode, this is the case if the O_z ions are moving away from (towards) the plane yielding an attractive interaction between the pair of electrons (holes) essentially in the region of the oxygens in the plane. This situation does not change qualitatively if the Cu-O polarizability is increased in our model. The only difference is that the changes of the potential at the Cu and $O_{x,y}$ now show different signs; however, the changes at $O_{x,y}$ having the same sign by symmetry dominate by far. Consequently the favorable situation for pair binding via the oxygens in the plane is improved.

We would like to note that the mechanism for pair binding related to the strong nonlocal electron-phonon interaction effects, based on the relatively poor screening by charge fluctuations of the changes of the Madelung-like potential induced by certain phonon modes, does not necessarily presume the existence of apical oxygen ions out of the planes.

From the characteristic properties of the screening mechanism, we find the following features to be relevant for the HTSC. The copper self-interaction U_d must remain large enough in order to suppress a charge-density wave instability in the system. The polarizability π should not increase too much in the metallic phase in order to guarantee the relatively poor screening via charge fluctuations [compare Eqs. (11) and (14)] of the changes of the Madelung potentials in the CuO plane provided by the displacements of the cations and anions, particularly those in the intergrown nonsuperconducting layers. Having these basic facts in mind, a particularly simple and effective system for HTSC should contain as key elements CuO planes alternating along the z axis with cation layers (without oxygen). The cations should be located above and below the centers of the copper squares of the CuO plane for stability reasons and to provide the attractive interaction for the pair in the region of the oxygens in an optimal way, as discussed above. A favorable situation could be achieved by variations of the composition of the cation layers resulting in certain variations of the lattice parameters of the system and thus of the Cu-O bond length and the cation oxygen bond length that, on the other hand, influence the values for $\tilde{V}$ and π as well as the strength of the changes of the Madelung potential in the plane. In this context it is interesting to note that in Ref. 31 the synthesis of such an "infinite-layer" parent compound of the superconducting system $A_2B_2Ca_{n-1}Cu_nO_{4+2n}$, with A = Tl,Bi and B = Ba,Sr, has been reported, namely $(Ca_{0.86}Sr_{0.14})CuO_2$. To our knowledge this system has not been made to superconduct as yet. Note also that our arguments are valid for both the design of electron-doped and hole-doped super-

conductors, so it is very likely that both types can be found by proper combinations of the content of the cation layers. Indeed, very recently the isostructural compound $(Sr_{1-x}Nd_x)CuO_2$ has been shown to be a 40 K superconductor of presumably electron-doped type[32] and in Ref. 33 the authors succeeded in making the "infinite layer" structure superconducting at 80 and 100 K in the Sr-Cu-O system. The sign of the carriers has not been determined until now.

Finally, we would like to comment that our ideas of a pairing mechanism reinforced by nonlocal, long-range electron-phonon interaction effects could also apply for the alkali-metal fullerides A_3C_{60}. Here we expect, on the basis of the arguments presented in this paper, a favorable situation for pairing, in particular via intramolecular symmetric breathing modes of the carbon balls vibrating at intermediate frequencies against the surrounding A^+ cations located at tetrahedral and octahedral sites, respectively, of the fcc lattice comprising the $(C_{60})^{3-}$ complexes (see for example, Refs. 34 and 35) and generating the poorly screened changes of the Madelung potential on the carbon balls during their vibrations, which are essential for our reasonings. The A^+ ion optical-phonon mode should play a minor role because of its low frequency and because the corresponding change of the Madelung potential on the carbon balls is of an alternating sign in this case.

IV. CONCLUSIONS

In this work we have pointed out the significance of nonlocal, long-range electron-phonon interaction effects of charge-fluctuation type for the phonon dispersion and the pairing mechanism in the high-temperature superconductors using La_2CuO_4 as an example. As shown in this paper, these effects are a consequence of the interplay of structure, strong ionic forces, and a special type of screening dominated by charge fluctuations and strong localization features of the electrons dictated by the Coulomb interaction. Some of our main results supporting these conclusions can be summarized as follows. The importance of the ionic forces is demonstrated by the calculation of the structural parameters and the phonon dispersion in a purely ionic *ab initio* model. The calculations have shown that important qualitative features of the ionic model, like the magnitude of the splittings of the E_u and A_{2u} modes, the relative position of the planar oxygen breathing mode, or the instability of the lattice with respect to the X point tilt mode are in agreement with the experimental facts. On the other hand, important features of the experimental dispersion, like the characteristic dip of the highest Δ_1 branch and at the same time, an increasing dispersion of the highest Σ_1 branch towards the X point, cannot be understood in an ionic model or by using the ideas of a standard screening approach for high-density metals. However, applying the proposed screening mechanism based on charge fluctuations and strong Coulomb effects, these features can be explained. For the insulating phase of La_2CuO_4, the charge fluctuations lead to a reduction of the E_u splittings in comparison with the ionic reference model. On the other hand, the discontinuities of the A_{2u} modes do not change at all. Also, the highest Λ_1 branch and in particular the O_z^z mode remains practically unchanged from the ionic model if a strictly two-dimensional electronic structure is assumed. This can be related to the fact that the charge transfer between the ions is locally restricted in this case within the CuO planes. This is in contrast to the metal, where we have shown that interplane charge-transfer processes lead to a large renormalization of O_z^z, as well as the highest Λ_1 branch, and to the vanishing of the A_{2u} discontinuity. As a result, we obtain a Λ_1 branch of very steep dispersion, also seen in the experiments. At the same time we obtain a flat dispersion all over along the considered directions in the Brillouin zone at about the frequency of O_z^z, which is optimal to achieve high T_c. Of course another drastic rearrangement of the phonon dispersion generated by the charge fluctuations in the metallic phase is the vanishing of the LO-TO splittings of the E_u modes. Finally, we have pointed out the relevance of the charge fluctuations accompanying the axial O_z- and La_z-breathing modes at the Γ and Z point, where in particular the O_z^z mode leads to changes of the potential in the CuO plane having the same sign at all the ions in the plane and generating a favorable situation for pair binding because two holes (electrons), can share a large, common region in space where they can lower their energy.

ACKNOWLEDGMENT

Financial support by the Deutsche Forschungsgemeinschaft Projekt No. Fa 170/2-1 is gratefully acknowledged.

[1]J. G. Bednorz and K. A. Müller, Z. Phys. B **64**, 189 (1986).
[2]W. E. Pickett, Rev. Mod. Phys. **61**, 433 (1989).
[3]R. E. Cohen, W. E. Picket, and H. Krakauer, Phys. Rev. Lett. **64**, 2575 (1990).
[4]J. Ranninger, Z. Phys. B **84**, 167 (1991).
[5]R. Zeyher, Z. Phys. B **80**, 187 (1990).
[6]C. Falter, Phys. Rep. **164**, Nos. 1 and 2 (1988).
[7]C. Falter, H. Rakel, and W. Ludwig, Phys. Rev. B **38**, 3986 (1988).
[8]M. Klenner, C. Falter, and W. Ludwig, Ann. Phys. (Leipzig, Heidelberg) **1**, 24 (1992).
[9]M. Klenner, C. Falter, and W. Ludwig, Ann. Phys. (Leipzig, Heidelberg) **1**, 34 (1992).
[10]P. B. Allen, in *Dynamical Properties of Solids*, edited by G. K. Horton and A. A. Maradudin (North-Holland, Amsterdam, 1980), Vol. 3.
[11]F. Herman and S. Skillman, *Atomic Structure Calculations* (Prentice-Hall, Englewood Cliffs, NJ, 1963).
[12]J. P. Perdew and A. Zunger, Phys. Rev. B **23**, 5048 (1981).
[13]R. E. Watson, Phys. Rev. **111**, 1108 (1958).
[14]R. G. Gordon and Y. S. Kim, J. Chem. Phys. **56**, 3122 (1972).
[15]R. E. Cohen, W. E. Pickett, H. Krakauer, and L. L. Boyer,

Physica B **150**, 61 (1988).
[16]J. M. Longo and P. M. Raccah, J. Solid State Chem. **6**, 526 (1973).
[17]W. Weber, Phys. Rev. Lett. **58**, 1371 (1987).
[18]L. Pintschovius, N. Pyka, W. Reichardt, A. Yu. Rumiantsev, A. Ivanov, and N. L. Mitrofanov (unpublished).
[19]L. Pintschovius, in *Phonons 89, Proceedings of the Third International Conference on Phonon Physics,* edited by S. Hunklinger, W. Ludwig, and G. Weiss (World Scientific, Singapore, 1990), Vol. 1.
[20]L. Pintschovius, N. Pyka, W. Reichardt, and A. Yu. Rumiantsev (unpublished).
[21]L. Pintschovius, N. Pyka, W. Reichardt, A. Yu. Rumiantsev, N. L. Mitrofanov, A. S. Ivanov, G. Collin, and P. Bourges, Physica C **185-189**, 156 (1991).
[22]L. Pintschovius (private communication).
[23]C. Falter, M. Klenner, and W. Ludwig, Phys. Lett. A **165**, 260 (1992).
[24]G. Vielsack and R. von Baltz, Phys. Status Solidi B **158**, 249 (1990).
[25]L. F. Mattheiss, Phys. Rev. Lett. **58**, 1028 (1987).
[26]J. Appel and W. Kohn, Phys. Rev. B **4**, 2162 (1971).
[27]L. J. Sham, Phys. Rev. **188**, 1431 (1969).
[28]R. M. Pick, M. H. Cohen, and R. M. Martin, Phys. Rev. B **1**, 910 (1970).
[29]A. Svane, Phys. Rev. Lett. **68**, 1900 (1992).
[30]J. P. Carbotte, Rev. Mod. Phys. **62**, 1027 (1990).
[31]T. Siegrist, S. M. Zahurak, D. W. Murphy, and R. S. Roth, Nature (London) **334**, 231 (1988).
[32]M. G. Smith, A. Manthiram, J. Zhou, J. B. Goodenough, and J. T. Markert, Nature (London) **351**, 549 (1991).
[33]Z. Hiroi, M. Takano, M. Azuma, Y. Takeda, and Y. Bando, Physica C **185-189**, 523 (1991).
[34]M. Schlüter, M. Lanoo, M. Needels, and G. A. Baraff, Phys. Rev. Lett. **68**, 526 (1992).
[35]F. C. Zhang, M. Ogata, and T. M. Rice, Phys. Rev. Lett. **67**, 3452 (1991).